

## **Experiments on Helicons in DIII-D – Investigation of the Physics of a Reactor-relevant Non-Inductive Current Drive Technology**

R.I. Pinsker<sup>1</sup>, R. Prater<sup>1</sup>, C.P. Moeller<sup>1</sup>, J.S. deGrassie<sup>1</sup>, C.C. Petty<sup>1</sup>, M. Porkolab<sup>2</sup>,  
J.P. Anderson<sup>1</sup>, J. Boedo<sup>3</sup>, Xi Chen<sup>1</sup>, A.M. Garofalo<sup>1</sup>, C. Lau<sup>4</sup>, A. Nagy<sup>5</sup>, D.C. Pace<sup>1</sup>,  
H. Torreblanca<sup>1</sup>, J.G. Watkins<sup>6</sup>, and L. Zeng<sup>7</sup>

email: pinsker@fusion.gat.com

<sup>1</sup>General Atomics, San Diego, California 92186-5608, USA

<sup>2</sup>Massachusetts Institute of Technology, Cambridge, Massachusetts 02139, USA

<sup>3</sup>University of California San Diego, San Diego, CA, USA

<sup>4</sup>Oak Ridge National Laboratory, PO Box 2008, Oak Ridge, TN 37831, USA

<sup>5</sup>Princeton Plasma Physics Laboratory, PO Box 451, Princeton, NJ 08543-0451, USA

<sup>6</sup>Sandia National Laboratories, PO Box 5800, Albuquerque, NM 87185-9052, USA

<sup>7</sup>University of California Los Angeles, PO Box 957099, Los Angeles, CA 90095, USA

**Abstract.** Experiments have begun in DIII-D to evaluate non-inductive current drive by Landau absorption of a toroidally-directed spectrum of helicon waves (also known as 'very high harmonic fast waves', 'fast waves in the lower hybrid range of frequencies', or 'whistlers'). Modeling has shown [1] that non-inductive current drive at mid-radius ( $\rho \sim 0.5$ ) should be achievable in DIII-D with fast waves at 0.5 GHz in high-beta conditions with an efficiency twice as high as with non-inductive current drive tools currently available on DIII-D (neutral beams and electron cyclotron current drive). An innovative Traveling Wave Antenna (TWA) of the 'comb-line' type with 12 radiating modules has been constructed, installed in DIII-D, and has been tested at very low power ( $< 0.4$  kW) to evaluate the antenna coupling in the linear regime, and to prototype technological aspects of such structures in the tokamak environment. Results show strong antenna/plasma coupling in several plasma regimes, most significantly in the high-beta ELMing H-mode case with calculated full first-pass absorption of the waves in the desired mid-radius region. No evidence of significant undesirable slow wave excitation was found when the total magnetic field adjacent to the structure was approximately aligned with the Faraday screen of the antenna. A high-power system is planned for installation in 2018 in which a single 1.2 MW klystron at 476 MHz will be used to power a TWA with  $\sim 30$  radiating elements in a structure  $\sim 2$  m wide. The goals of the high-power experiments include evaluation of non-linear effects on excitation of the desired waves (ponderomotive effects, parametric decay) and measurements of the deposition profile and the current drive efficiency.

### **1. Introduction**

Design studies [2] have shown that steady-state tokamak reactors require efficient non-inductive current drive in the mid-radius region. While the quasi-electrostatic slow wave in the Lower Hybrid Range of Frequencies (LHRF), usually called the 'lower hybrid wave', can be used to drive current near the edge of a reactor plasma, whether or not the current can be driven in the core plasma is still a topic of active investigation [3]. Here we consider the application of the other wave polarization in the LHRF, which is the quasi-electromagnetic fast wave, sometimes called the 'whistler' or 'helicon' wave [4]. Like the slow wave, the helicon in this regime interacts with electrons with high parallel phase velocity, so that trapping in the inhomogeneous toroidal magnetic field can be less of an issue for these waves than for current drive using waves in the Electron Cyclotron Range of Frequencies. But comparing the slow and fast wave in the LHRF, the electron damping of the fast wave is weaker than that of the slow wave at the same frequency and parallel wave number, which permits better penetration into the core and current drive in the desired mid-radius region with the fast wave.

Current drive using the helicon is lacking an experimental basis to date, because in previous experiments [5] the single-pass electron damping was weak (low electron temperature, low density) so that many passes through the plasma would have been required to damp the wave, with

accompanying loss of spectral control, and the possibility of mode-conversion and subsequent absorption as slow waves. Previously, current drive with fast waves in the medium-to-high ion cyclotron harmonic regime was demonstrated in DIII-D [6] at frequencies up to 120 MHz. The present effort will extend the investigation to the range of very high ion cyclotron harmonics (i.e. the LHRF) regime. A crucial aspect of this regime is the challenge of an appropriate wave-launching structure. To obtain electron Landau damping, waves with an index of refraction parallel to the static magnetic field greater than unity ( $n_{\parallel} > 1$ ) must be excited. Such waves are radially evanescent in the vacuum region adjacent to the wave launcher. The radial decay rate at a given  $n_{\parallel}$  increases with frequency, so the coupling per unit area of wave launcher must necessarily be weak in the LHRF. A necessary (though not sufficient) condition for a suitable structure is that sufficient coupling be obtained in the linear regime for plasmas with plasma edge conditions like those in the desired target plasmas for the subsequent high-power system. 'Sufficient coupling' means that the antenna electric fields projected to the high power system would nowhere exceed limits for electric breakdown at the desired coupled power level.

In this work, we describe the measured properties of a prototype wave-launcher for fast waves in the LHRF installed in the DIII-D tokamak. We measure the antenna coupling at very low applied power levels (linear regime),  $< 0.4$  kW at 476 MHz, under a wide range of discharge conditions. Good coupling to the plasma is found in target plasmas that are calculated to have full absorption of the applied power in the desired mid-radius region of the plasma core.

## 2. Comb-line Traveling Wave Antenna: Low-power Antenna Design, Construction, Installation, Diagnostics

The design of the wave-launching structure chosen for this experiment is a traveling-wave antenna of the 'comb-line' type [7,8]. This comb-line consists of a toroidal array of modules, each of which is fed via mutual reactive coupling from its 'upstream' neighbor, with only the end element at the upstream end actively fed via a feedthrough. The element at the 'downstream' end is also equipped with a feedthrough so that any remaining uncoupled power is taken out of the antenna rather than allowing it to reflect back upstream, which would degrade the directivity of the launched spectrum. Since the modules other than the end ones are identical and do not have feedthroughs, the antenna has a shallow radial build and is a modular design that can be extended to any toroidal length (number of modules) needed to compensate for weak coupling to the plasma per element. A simple lumped-element model of such an array (Fig. 1) shows that the structure acts as a band-pass filter, with the center of the pass-band at the LC resonant frequency of each element and the phase difference from an element to the next of  $\pi/2$  at the center of the band. The bandwidth is determined by the ratio of the mutual inductance to the self-inductance of an element; at the lower (upper) band edge, the phase difference approaches 0 ( $\pi$ ).

The resistance of each element represents the sum of the skin effect resistive loss and the loading resistance representing energy lost to waves propagating away from the antenna in the plasma. Were there no

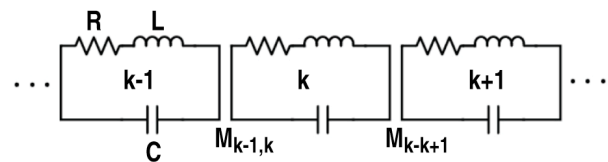


FIG. 1. Simple lumped-element model of comb-line traveling wave antenna. Resulting power transmission coefficient at mid-band neglecting end effects is  $|T|^2 \approx [1 - R/(4\pi f_0 M)]^{2n}$ , where  $n$  is the number of elements,  $R$  is the resistive loading (sum of wave loading and resistive losses) per module and  $M$  is the net mutual reactance coupling currents in one module to those in the next.

resistive loss in the structure, all of the applied power could be coupled to the plasma regardless of how low the loading resistance per element would be by adding more modules to the array - the weaker the coupling to the plasma, the longer the required array. But in the realistic case in which the resistive loss in each element is non-zero, a minimum load resistance per element is needed to couple a specified fraction of the power applied to one end of the structure to the plasma. The minimum acceptable coupling to the plasma is thus determined by how much the resistive losses can be reduced. For the low-power prototype comb-line, the main purpose was to measure the plasma coupling (i.e., the loading resistance) in a variety of tokamak discharge conditions, so that little effort was made to minimize the resistive losses for the prototype.

The design of the individual modules in the structure was somewhat more complex than in the 200 MHz comb-line built for JFT-2M previously [8], in that the allowed poloidal length in this case of about 0.21 m would have been wasted had the current strap consisted of only a single quarter-wave-long segment (at 476 MHz, one quarter wavelength = 0.1575 m). Hence the module consists of essentially a stack of two elements, mirror-symmetric about the midplane of the module. Initial computational studies showed that the peak rf electric field in the end-loading capacitances would be rather high in the subsequent 1 MW antenna, so each half of the module was split again into a pair of modules (reducing the peak electric field in the capacitors for a given power level by a factor of 0.707), leading to the final design of a poloidal stack of four short straps, each equipped with a capacitor at the high voltage end of the 'straplet'. To excite the appropriate resonance, in which the currents in all four straplets are in phase, thereby exciting the poloidal mode number spectrum peaked at 0, it is necessary to feed the two inner straplets out of phase on the end element. The end elements (the topmost and bottom-most of the four) are fed primarily via the mutual reactance to the inner pair, with a bar at the back of the element connecting the capacitor plates together to separate the desired in-phase resonance from the (undesired) out-of-phase resonance. The resulting module is shown in the left-most panel of Fig. 2, where part of the Faraday screen has been removed to show half of the strap design. The poloidal length of each module is approximately 0.21 m and the toroidal width is 0.05 m. (With this toroidal width of a single module, the array excites a spectrum peaked at  $n_{||}=3$  at midband, at 476 MHz.) The height (radial extent) of the module is about 0.077 m. The module body is constructed from Cu-Cr-Zr high-strength alloy, and the Faraday screen elements are fabricated from Ti-Zr-Mo (TZM), coated with a thin layer ( $\sim 25\text{-}50\ \mu\text{m}$ ) of boron carbide.

The twelve modules of the prototype antenna were mounted on a stainless-steel plate at an angle of 16 deg from vertical so that for one choice of helicity of the total static magnetic field (toroidal plus poloidal), the current-carrying straplets are approximately perpendicular to the static magnetic field lines adjacent to the antenna, in an effort to minimize the direct excitation of the slow wave

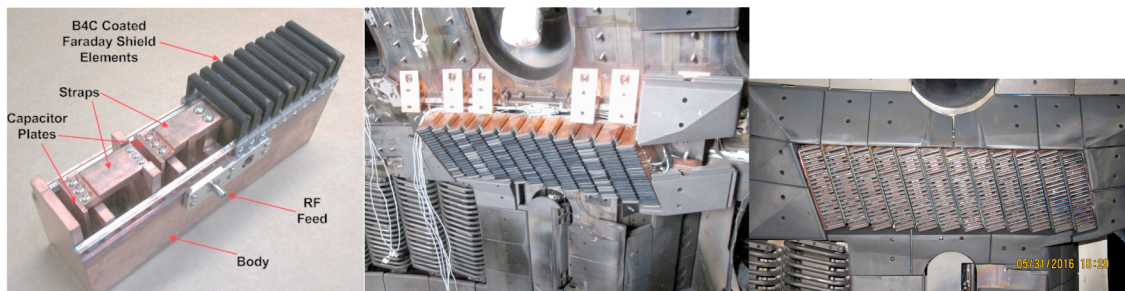


FIG. 2. (a) Photograph of a single module with half of the Faraday screen removed, showing two of the four poloidal LC circuits in each module. (b) Installation of the 12 modules in DIII-D, with diagnostic cables visible at left end and two protective graphite tiles at right. (c) Completed installation after operation for five months in DIII-D.

polarization. By comparing the antenna loading with optimized alignment to that measured in the relatively poor alignment that exists with the opposite helicity (reversing the sign of the toroidal field while keeping the direction of the plasma current fixed), the slow wave loading that would be expected in the latter case might be manifest as a larger total loading than in the case of optimized alignment. This, however, would require that the edge parameters, in particular the scrape-off layer (SOL) density profiles, to be identical in the two cases, which may not be the case due to the lack of up-down symmetry of the structures on the first wall in the vacuum vessel. Given that the antenna was mounted at a height of 0.3 m above the midplane, the up-down asymmetry with respect to the antenna is evident. The mounting plate was supported by copper wedges attached to the Inconel vacuum vessel wall in order to conduct heat from the antenna to the water-cooled vessel surface. The antenna was surrounded by graphite tiles to protect the antenna from fast ion losses from unconfined neutral beam particles. Photos showing the antenna during the installation and of the completed installation after five months of plasma operations are shown in Fig. 2 (b) and (c). Design studies of the fast ion deposition on the antenna and surrounding structures are described in [9].

The twelve modules were assembled on the bench and the electrical properties of the antenna without load were measured with a network analyzer prior to their installation in DIII-D. The transmission coefficient from one end feed to the other ( $S_{21}$ ) as a function of the applied frequency was found to have the expected band-pass filter characteristic, as plotted (green curve) in Fig. 3(a). The input reflection coefficient of the feed at either end ( $S_{11}$ ,  $S_{22}$ ) is low ( $< 0.2$  in amplitude = 4% in power) throughout the  $\sim 20$  MHz bandwidth centered on 476 MHz [Fig. 3(b)]. Since the antenna does not excite waves that propagate in vacuum (i.e., with  $n_{\parallel}^2 < 1$ ), the extent to which the measured transmission coefficient magnitude is less than unity in the center of the pass-band is a measure of the resistive losses in the structure. These losses were found to be larger than had been expected based on previous prototypes. Losses due to the boron carbide coating on the Faraday screen rods or due to finite resistance of the joints in the structure, both aspects of which were different in the earlier prototypes, may be responsible for the larger-than-expected resistive losses.

The measurements were repeated after the modules were mounted in DIII-D, and the transmission coefficient is shown as the dotted red curve in Fig. 3(a), this having been corrected for the losses in the small diameter vacuum-compatible 50 Ohm semi-rigid coaxial cables used to transmit the power from the feedthroughs on the tokamak to the feeds of the antenna. The installation on the tokamak not being identical to the bench measurement (toroidal curvature of the mounting plate, etc.) would be expected to result in slight differences between the bench and the corrected mounted measurements, as is visible in the figure.

The comb-line was equipped with multiple diagnostics. The primary rf measurements were of the forward, reflected and transmitted power, determined with directional couplers and a heterodyne detection system in which the signals at 476 MHz were mixed down to 100 kHz and then digitized at

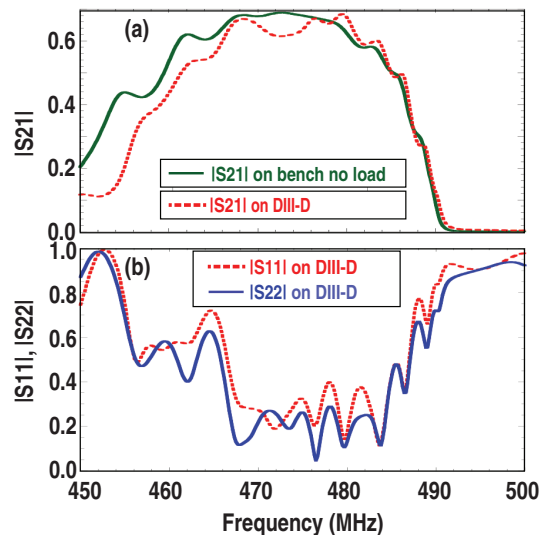


FIG. 3. (a) Transmission coefficient through the twelve modules on the bench (green) and in DIII-D (red) as a function of frequency over the passband centered at 476 MHz. (b) Input reflection coefficient of structure as a function of frequency, fed from either end, with a good impedance match to the  $50 \Omega$  feedline in the passband.

1 MS/sec with a simultaneously sampling digitizer. Each module has a built-in one-turn rf magnetic probe to measure the amplitude and phase of the current in the module, the cables to which can be seen on the left of Fig. 2(b) during installation. These signals were acquired and processed with the same heterodyne system. Seven thermocouples were installed at various points in the comb-line modules and four more were placed in the surrounding graphite tiles in order to quantify the heating of the antenna components from fast ion deposition. A single Langmuir probe was placed in one of the tiles adjacent to the antenna to measure the electron density in the immediate neighborhood of the Faraday screen. Pre-existing diagnostics that were of particular interest in this study included a profile reflectometer at the midplane, which was used to measure the edge density profiles that determine the antenna loading, Thomson scattering, which also provided edge density information, a wide-viewing infrared camera that was used to further quantify heating of the antenna, and a mid-plane reciprocating Langmuir probe, which could provide SOL density measurements in discharges at low neutral beam power.

### 3. Measured Properties with Plasma Load

Since the radial exponential decay length of the antenna fields in the vacuum region adjacent to the antenna is only 3.5 cm, and the distance between the last closed flux surface of typical DIII-D plasmas and the outer wall where the antenna was installed is typically much larger, it was necessary to have the antenna face and surrounding protective graphite tiles at that elevation protrude from the outer wall. Hence, it was important to determine whether the antenna would survive the heat flux of discharges with high neutral-beam heating power levels, or otherwise reduce the DIII-D operating space. Initial experiments showed that only minor restrictions on the plasma shape were needed; these restrictions were enforced by the digital plasma control system automatically during the campaign during which the comb-line was present. Additionally, simulations and experiment [9] showed that it was necessary to limit the amount of energy injected from a particular neutral beam (the '210L' source) when the direction of the toroidal field was reversed from the more common direction for DIII-D operation to avoid overheating of the antenna modules at one end of the structure from fast ion losses. As is faintly visible in Fig. 2(c), the right edge of the antenna and the surrounding tiles did show signs of significant heat deposition even with the constraints in place. However, during the five-month period of operation with the antenna installed, no excessive impurities or other deleterious effects on the discharges related to the presence of the antenna were observed, indicating that the restrictions were sufficient.

As with any kind of wave-launching structure in the ICRF or the LHRF, the resistive loading is primarily determined by the radial distance between the face of the wave-launcher and the cut-off layer where the wave begins to propagate (in this case, at a density on the order of  $1.4 \times 10^{18} \times B_T \text{ m}^{-3}$ , where  $B_T$  is the local magnetic field in T) and secondarily, on the value of the density gradient in the neighborhood of the cut-off (the 'dielectric mirror' effect). Since this density range occurs in the far SOL, these parameters, and hence the resistive loading, are strongly dependent on the confinement regime (L-mode, H-mode), details of the level of gas puffing vs. active pumping, wall conditions, etc. The comb-line antenna loading was measured throughout the discharge by applying up to 0.4 kW to one end of the structure at a fixed frequency (usually 476 MHz), starting 1 second before the plasma current initiation and ending after 4 seconds of the discharge, and recording the forward, reflected, and transmitted power levels and the rf probe signals from the 12 internal magnetic loops. The loading was characterized by the ratio of the rf current in the  $n$ th antenna module to that in the

( $n+1$ )th module, which was deduced directly from the rf probe signals or from the end-to-end transmission coefficient  $S_{21}$  as  $|S_{21}|^{(1/12)}$ , in which case it is a value averaged over the antenna. The probe signals showed that the assumption of uniformity among modules was a good one, and these two methods of measuring the module-to-module amplitude decay factor (henceforth referred to as  $\delta_a$ ) agreed well over a wide range of loading levels, as shown in Fig. 4. The lightest possible loading, i.e.,  $\delta_a$  closest to unity, is obtained without plasma load, and the heaviest loading is observed in L-mode plasmas with a small gap between the comb-line traveling wave antenna and the last closed flux surface, which we call TWAGAP.

If we assume that the distance from the last closed flux surface to the cut-off layer remains fixed as TWAGAP is varied, we can compare the rate of decay of the loading as TWAGAP grows with the simplest theoretical expectation. Also assuming that the launched  $n_{||}$  spectrum is sharply peaked at  $n_{||}=3$ , we predict that the resistive loading should decrease with TWAGAP with an exponential decay length of half of the amplitude decay length, i.e. 1.75 cm. Dynamic gap scans were carried out in otherwise steady L-mode (inside-wall-limited and in double-null-divertor topologies) and in H-mode discharges before the first ELM, with the results plotted in Fig. 5. Also shown is the loading in an ELMing H-mode with a TWAGAP scan, measured between ELMs. What is plotted on a logarithmic ordinate is the difference between  $\delta_a$  in vacuum and the measured value of  $\delta_a$  in plasma, which is proportional to the part of the resistive antenna loading due to wave excitation. It can be shown that this quantity should decay with the characteristic length of 1.75 cm under the set of assumptions listed above. Though this simple model does predict an exponential decay with a single characteristic length, which is supported by the data, the fits indicate a nearly a factor of two slower decay of the loading with TWAGAP than expected. This discrepancy suggests that at least one of the assumptions of the simple model must be invalid. However, from a practical standpoint, this relatively slow decay of the loading as the antenna/plasma distance increases is very favorable for projections to a high-power antenna, in that the antenna can be positioned at a larger radial distance from the plasma than originally envisioned and still couple the power desired without challenging breakdown limits in the antenna.

Unintended excitation of the quasi-electrostatic slow wave as a result of residual rf electric fields parallel to the total static magnetic field lines was a concern and a topic of investigation in this experiment. The cut-off density for the slow wave at this frequency (where the applied frequency equals the electron plasma frequency) is very low, about  $3 \times 10^{15} \text{ m}^{-3}$ . This density would be expected to exist very near the face of the antenna, so the excitation of slow waves by any residual  $E_{||}$  would

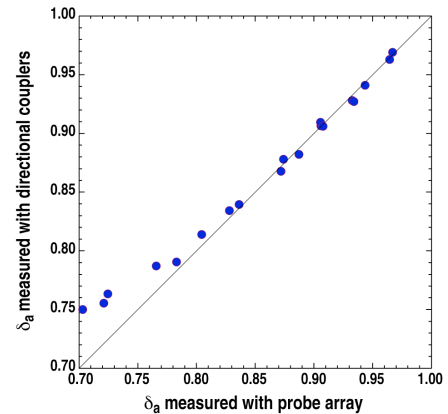


FIG. 4. Excellent agreement is obtained between two independent measurements of  $\delta_a$ .

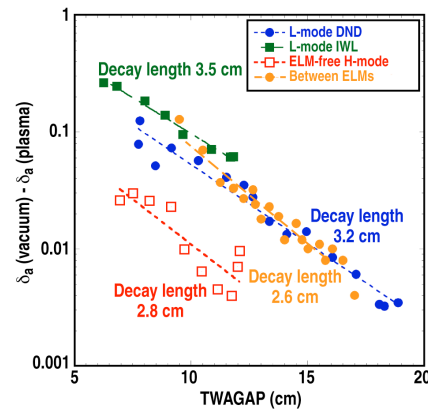


FIG. 5. Decay of antenna loading as the plasma/antenna gap is increased in four regimes: L-mode in inside-wall-limited ohmic discharge (green squares), L-mode in double-null-diverted discharge (blue filled circles), H-mode prior to the first ELM (open red squares) and between ELMs in an ELMing H-mode (filled orange circles).

be expected to be efficient. If the resistive loading due to slow wave excitation is non-negligible, we expect a minimum in the resistive loading when the static magnetic field lines are precisely aligned with the Faraday screen elements (perpendicular to the current in the straplets) [10]. Experiments were performed in which the local magnetic field line pitch angle was varied by ramping the plasma current and/or the toroidal field during the discharge and the resistive loading measured during the scan. No resonant minimum loading feature was observed in the neighborhood of perfect alignment. Also, the loading was compared in up-down symmetric discharges with as nearly identical engineering parameters as possible with the only difference being the sign of the toroidal field (at a fixed direction of plasma current). The slight differences in the resistive loading between these cases, one with nearly perfect alignment and one with maximum misalignment ( $\sim 30$  deg), may have been due to small observed differences in recycling at various places in the vessel, not due to wave physics.

A simpler way to observe unintended slow wave loading is to increase the plasma/antenna gap to a large value and compare the minimum loading to the vacuum loading. The expectation, especially in L-mode plasmas, is that the density very near the antenna would remain above the slow wave cutoff density even at a very large value of TWAGAP (at which the coupling to the fast wave would be exponentially small), so that at such large gaps the loading would remain observably larger than the vacuum value due to the slow wave excitation. The blue filled circles in Fig. 5 show that in a double-null-divertor L-mode plasma, the loading smoothly approaches a value indistinguishable from the vacuum value at very large values of TWAGAP, rather than asymptotically approaching a minimum value above the vacuum level. This places an upper limit on the fraction of slow wave to total (slow wave plus fast wave) excitation at the particular value of field line misalignment, only a few degrees in this case. Hence we conclude that the antenna does not excite slow waves significantly, at least for reasonably good field line/Faraday screen alignment.

The planned high-power ( $\sim 1$  MW) follow-on experiment to these low-power coupling measurements will use a particular target plasma that was identified [1] from the DIII-D database that has essentially complete single-pass absorption of the helicon wave launched at  $n_{||}=3$  at mid-radius. The practical question addressed in the low-power prototype comb-line experiments was whether the resistive loading of the antenna in this particular regime is high enough to permit coupling of sufficient power with a high-power version of the comb-line. The numeric goal was to determine whether a 30-element comb-line would be able to couple 75% of the applied power to the plasma in one pass through the antenna in this regime. The high-power version of the comb-line would need to have lower resistive losses than the prototype, so the presumed level of resistive losses was set

to a value considered to be practically achievable (bench tests of new prototype modules will demonstrate this level of loss in the near future.) Given that the lower resistive loss is successfully attained, to achieve the desired 75% coupling to the plasma corresponds to a value of  $\delta_a$  for the prototype of 0.925. The target discharge was reproduced and the loading measured throughout the

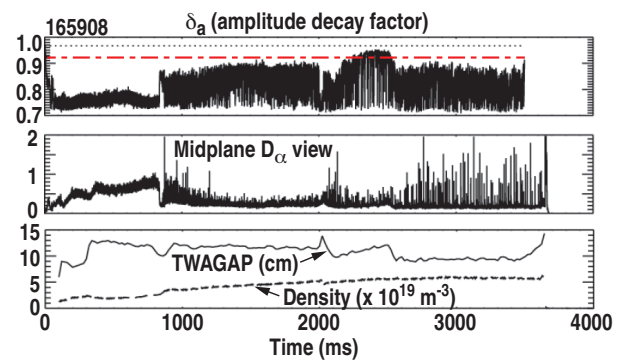


FIG. 6 Coupling observed in an ELMing H-mode with projected complete first-pass off-axis absorption of the coupled power is sufficient at almost all times during the discharge (below the dashed red line in the upper box) to yield  $> 75\%$  of the applied power coupled to the plasma, assuming a 30-element antenna with reduced vacuum losses.

discharge, as shown in Fig. 6, where the critical level of  $\delta_a$  is indicated as a dashed red line. The measured value of resistive loading is higher than the minimum required ( $\delta_a$  is below the dashed red line) for the entire discharge, except for a short period after 2 sec, even between ELMs. Hence, we may conclude that the comb-line antenna projects to a successful high-power experiment, if the required lower resistive losses can be achieved.

#### 4. Conclusions

The comb-line traveling wave antenna has been shown to couple well to a broad range of DIII-D discharges. In particular, the antenna loading in the principal target discharge for the high-power experiment should permit ~75% of the power applied to the antenna feed to be coupled to the plasma in a 30-element version of the comb-line. No evidence has been found of significant parasitic direct excitation of slow waves, at least under conditions with reasonably good alignment between the Faraday screen elements and the static magnetic field lines near the antenna.

The outlook is therefore positive for 1 MW-level follow-up experiments, which will permit addressing non-linear aspects of wave excitation (e.g., ponderomotive effects, parametric decay instabilities, scattering from density fluctuations leading to 'stimulated mode conversion' [11], etc.) and should lead to measurement of the non-inductive current drive efficiency for this reactor-relevant current drive technique. Linear modeling predicts [1] an rf-driven current of ~60 kA per coupled MW of helicon power, which should result in an easily measurable driven current in DIII-D in high-beta discharges like the target plasma studied in this work, so that the effect of non-linear behavior will be quantitatively assessed by measuring the deviation of the driven current from the linear predictions.

#### Acknowledgement

This material is based upon work supported in part by the U.S. Department of Energy, Office of Science, Office of Fusion Energy Sciences, using the DIII-D National Fusion Facility, a DOE Office of Science user facility, under Awards DE-FC02-04ER54698<sup>1</sup>, DE-FG02-94ER54084<sup>2</sup>, DE-FG02-07ER54917<sup>3</sup>, DE-AC05-00OR22725<sup>4</sup>, DE-AC02-09CH11466<sup>5</sup>, DE-AC04-94AL8500<sup>6</sup>, and DE-FG02-08ER54984<sup>7</sup>. DIII-D data shown in this paper can be obtained in digital format by following the links at [https://fusion.gat.com/global/D3D\\_DMP](https://fusion.gat.com/global/D3D_DMP).

#### References

- [1] PRATER, R., et al., Nucl. Fusion **54**, 083024 (2014)
- [2] JARDIN, S.C., et al., Fusion Eng. Design **38**, 27 (1997)
- [3] CARDINALI, A., et al., in *Radio Frequency Power in Plasmas (Proc. 21st Topical Conf., CA, USA, 2015)* (AIP, Melville, NY) 030015
- [4] PINSKER, R.I., Phys. Plasmas **22**, 090901 (2015)
- [5] PINSKER, R.I. in *Radio Frequency Power in Plasmas (Proc. 10th Topical Conf., Boston, MA, 1993)* (AIP, Melville, NY) p. 179
- [6] PETTY, C.C., et al., Plasma Phys. Control. Fusion **43**, 1747 (2001)
- [7] MOELLER, C.P., et al., in *Radio Frequency Power in Plasmas (Proc. 10th Top. Conf., Boston, MA, 1993)* (AIP, Melville, NY, 1994) p. 323
- [8] PINSKER, R.I., et al., in *Fusion Technology 1996 (Proc. 19th Symp., Lisbon, Portugal, 1996)* (Elsevier, Amsterdam, 1997) p. 629
- [9] PACE, D.C., et al., Fusion Eng. Des. **112**, 14 (2016)
- [10] PINSKER, R.I., et al., in *Radio Frequency Power in Plasmas (Proc. 21st Topical Conf., CA, USA, 2015)* (AIP, Melville, NY) 080012
- [11] ANDREWS, P.L., Phys. Rev. Lett. **54**, 2022 (1985)